

Monte Carlo study of the **XY**-model on Penrose lattices

This article has been downloaded from IOPscience. Please scroll down to see the full text article.

1998 J. Phys.: Condens. Matter 10 2303

(<http://iopscience.iop.org/0953-8984/10/10/012>)

View [the table of contents for this issue](#), or go to the [journal homepage](#) for more

Download details:

IP Address: 171.66.16.209

The article was downloaded on 14/05/2010 at 16:15

Please note that [terms and conditions apply](#).

Monte Carlo study of the XY -model on Penrose lattices

R W Reid, S K Bose and B Mitrović

Physics Department, Brock University, St Catharines, Ontario L2S 3A1, Canada

Received 24 June 1997, in final form 13 January 1998

Abstract. We have carried out a Monte Carlo study of the nearest-neighbour ferromagnetic XY -model on the two-dimensional (2D) Penrose lattice and on periodically stacked (three-dimensional) 2D Penrose lattices. For the 2D case we have examined the magnetization, specific heat, linear susceptibility, helicity modulus and the derivative of the helicity modulus with respect to inverse temperature. The behaviour of all of these quantities points to a Kosterlitz–Thouless transition occurring in the temperature range $T_c = (1.0\text{--}1.05)J/K_B$, with critical exponents that are consistent with those obtained for crystalline (e.g., square) lattices. For the 3D stacking of the 2D Penrose lattices, examination of the magnetization, specific heat and linear susceptibility reveals a conventional second-order phase transition. Through cumulant analysis and finite-size scaling we obtain a critical temperature $T_c = (2.292 \pm 0.003)J$ and critical exponents $\alpha' = 0.03 \pm 0.03$, $\beta = 0.30 \pm 0.01$ and $\gamma = 1.31 \pm 0.02$, in agreement with previous studies of the XY -model on the 3D cubic lattice.

1. Introduction

The effect of the unique structural properties of quasicrystals, such as quasiperiodicity, hierarchical length scales and self-similarity, on phase transitions and critical phenomena has not yet been studied at length. Arguments have been presented to the effect that quasiperiodic or ‘limit quasiperiodic’ structures that are characterized by bounded fluctuations in structural features (also described as *Pisot structures*) belong to the same universality class as crystals or periodic structures [1]. A similar argument applies to aperiodic structures as well. Thus, in the language of the renormalization group, both aperiodicity and quasiperiodicity appear irrelevant. So far, this seems to be supported by numerical simulations on planar Penrose tilings for the Ising model [2], percolation problem [3] and random and self-avoiding walks [4]. Sorensen *et al* [2], in particular, have analysed the Ising model data for a sequence of periodic rational approximants of the 2D Penrose lattice, each characterized by an integer q such that the limit $q \rightarrow \infty$ yields the quasiperiodic Penrose lattice. By extrapolating the results for the rational approximants they rule out the possibility of a change in the universality class as $q \rightarrow \infty$, i.e. for the truly quasiperiodic case. A version of the eight-vertex model on the Penrose lattice has been solved by Korepin [5] and is found to have critical properties close to the periodic case.

In this work, we present a detailed Monte Carlo study of the ferromagnetic nearest-neighbour XY -model on 2D Penrose lattices [6] and a periodic 3D stacking of such lattices, with results indicating that quasiperiodicity is indeed an irrelevant variable for this model. The first part of our study, involving 2D Penrose lattices, closely follows that of Tobochnik and Chester [7], Van Himbergen and Chakravarty [8], Teitel and Jayaprakash [9] and Shih and Stroud [10] on square lattices. A study of the XY -model on the 2D Penrose lattice,

including up to third-nearest-neighbour interactions, has been reported by Ledue *et al* [11]. These authors studied the magnetic properties of the model for different relative signs and magnitudes of the three near-neighbour interactions. Among other findings, they reported the existence of a Kosterlitz–Thouless (KT) [12, 13] transition for which evidence was provided via the thermal variation of the specific heat and, in particular, the saturation of the specific heat peak with increasing system size. However, details of the KT transition, such as the critical exponents and the transition temperature itself, were not determined. In this work, the KT transition on a Penrose lattice is studied in detail, with calculations of the specific heat, susceptibility, magnetization, helicity modulus and the derivative of the helicity modulus with respect to inverse temperature.

We also examine a 3D version of our model, namely, the 2D Penrose lattices stacked periodically along the z -direction. Previous MC studies of the 3D XY -model on cubic lattices, performed by Hasenbusch and Meyer [14], Janke [15] and Gottlob and Hasenbusch [16], have all revealed the usual second-order transition. Our systems exhibit a critical behaviour similar to that reported in the above studies on cubic lattices. Using a cumulant analysis we determine the critical temperature, and then perform a finite-size scaling of the magnetization, susceptibility and specific heat. The critical exponents that we obtain are in good agreement with the accepted values [17].

A couple of comments about the choice of our 3D systems are in order. A natural extension of our 2D system would be a 3D Penrose lattice (Amman tilings). On the basis of the universality hypothesis one would expect the 3D Penrose lattice to show a similar transition and exponents to the periodically repeated 2D tilings we have considered. However, since the spin configurations in the XY -model are two dimensional, the model is more suitable for describing interactions in planar structures than non-planar ones. 3D Amman tilings exhibit no planar structure, inasmuch as there are no clearly identifiable sets of parallel planes along which the spins would have any physical grounds for lying. From this point of view, our choice of the 3D systems seems more natural for the XY -model. In addition, the 3D systems that we have studied are known to form the lattices that describe decagonal quasicrystals, structures that show quasiperiodicity in the XY -plane, but are periodic along the z -direction. For example, the decagonal Al–Cu–Co quasicrystal is described quite well by the Burkov model [18] where the vertices and the interstitials of a 2D Penrose lattice are decorated with certain atomic motifs and the resulting 2D structure is repeated periodically in the perpendicular (z -) direction. A third reason for studying the periodic stacking of 2D Penrose lattices is that it would allow us to study the crossover from the KT to the normal second-order transition as the number of layers is increased beyond one. Although the KT transition is deemed to be unique to two dimensions, the details of the change in the nature of this transition as the dimensionality is increased beyond one have not been studied. We are currently engaged in this study, and hope to be able to report on it in the near future. Since this study is currently incomplete we prefer to refrain from making any comments on the above crossover phenomenon in the present paper.

The remainder of this paper is divided into sections as follows. In section 2 of this paper we discuss our model and some details of the MC calculation. In sections 3 and 4 we present the results for the 2D and the 3D systems, respectively. In section 5, we present our comments and conclusions.

2. The model and the simulation

We consider each vertex i of a finite lattice to be occupied by a classical XY -spin S_i of unit magnitude, at an angle θ_i with respect to a fixed reference line. We also suppose that two

spin vectors with orientations θ_i and θ_j situated at lattice sites i and j interact via a nearest-neighbour coupling parameter J . The Hamiltonian for this system (the nearest-neighbour ferromagnetic XY-model) is thus given by

$$H = -J \sum_{[ij]} \mathbf{S}_i \cdot \mathbf{S}_j = -J \sum_{[ij]} \cos(\theta_i - \theta_j) \quad (1)$$

where the summation is restricted to nearest-neighbour pairs $[ij]$. To study the statistical mechanics of this model we have used MC simulations based mainly on the Metropolis algorithm [19], but occasionally the cluster spin algorithm of Wolff [20], and Ferrenberg and Swendsen [21] was also used.

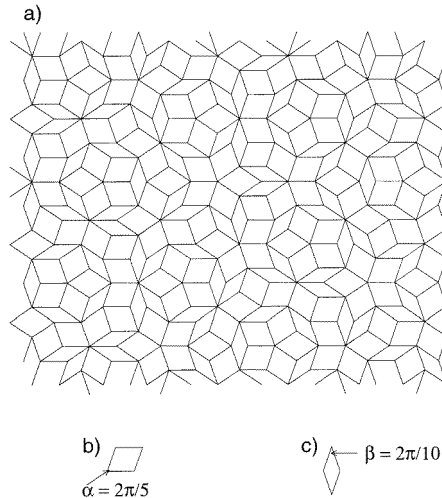


Figure 1. (a) A section of a Penrose lattice, composed of two basic unit cells: (b) the fat rhombus and (c) the thin rhombus.

In figure 1(a) we show a section of a 2D Penrose lattice [6], composed of two basic unit cells, the ‘fat’ and ‘thin’ rhombuses shown in figures 1(b) and 1(c). The coordination number for a lattice point in the Penrose lattice varies between 3 and 7, but has an average value of 4 as in a square lattice. The ring structure is also similar to that of a square lattice, i.e. only even-order rings appear. The self-similarity, or equivalently the inflation–deflation property, of the Penrose lattice is governed by an irrational number, the Golden Mean ($\tau = (1 + \sqrt{5})/2$), which also dictates its decagonal (pentagonal) bond-orientational order. In our finite-cluster MC simulations, we have used periodic boundary conditions in order to reduce surface effects. Rational approximants of the 2D Penrose lattice, which can be repeated periodically, can be obtained from a sequence of rational (Fibonacci) approximations to the Golden Mean. We follow a systematic way of generating these periodic or rational approximants of the Penrose lattice, as given by Lançon and Billard [22]. For the rest of this paper, we will refer to these approximants as periodic Penrose lattices (PPL).

During the simulation the 2D and 3D systems were heated and cooled in a quasistatic fashion, with quantities calculated only after equilibration had been achieved at each temperature. This was determined by monitoring the internal energy and specific heat every 10 to 100 steps per particle (spp). Typically, equilibration required 2000–8000 spp. Averages were then calculated over M blocks, with a standard deviation (divided by $\sqrt{M - 1}$

as opposed to \sqrt{M} used to determine the error. A grand average was then performed over the cooling and heating data.

Table 1. The number of sites and linear dimensions of the 2D PPLs used in the simulation.

N	L_x	L_y
644	24.80	21.09
1686	40.12	34.13
4414	64.92	55.23
11 556	105.05	89.36

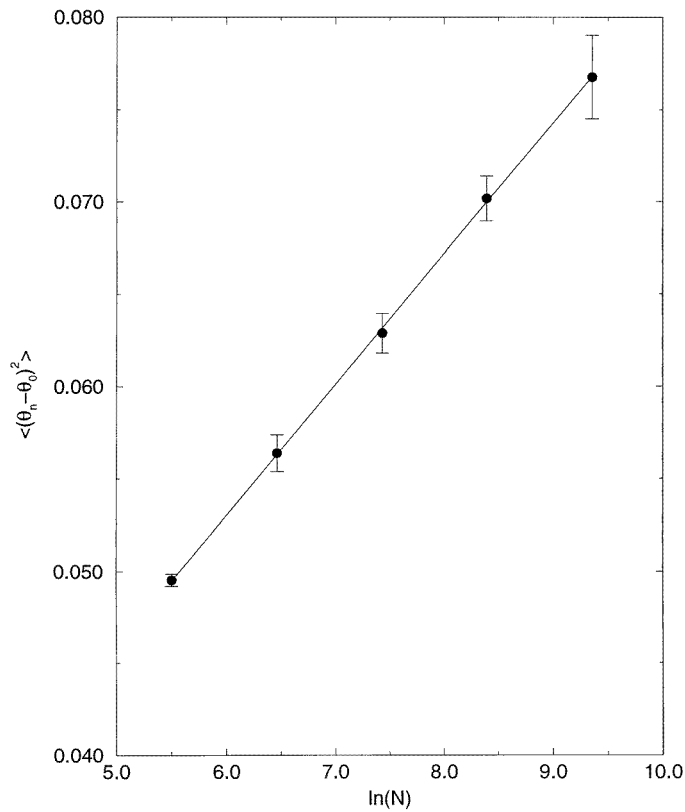


Figure 2. The ASD versus $\ln N$ at $T = 0.1J$ in 2D Penrose lattices. The straight line is a least-squares fit of the data.

3. 2D systems

For the 2D systems, we have examined the mean square angular displacement $\langle\theta^2\rangle$, linear susceptibility χ , specific heat C and helicity modulus γ . Simulations were carried out on PPLs with 246, 644, 1686, 4414 and 11 556 sites. In table 1, we present the linear dimensions of these N -site clusters in the conventional x - and y -directions, L_x and L_y

respectively. Starting from a completely ordered state ($T = 0$), the systems were heated up to a temperature of $T = 2.0J$ and then cooled back down.

All previous work done on periodic lattices (square, triangular and honeycomb) [7–10] points to a KT transition ([12, 13]; see also [23]). Although the square-lattice results give varying values for the critical temperature ($T_c = 0.89$ – $0.95J$) and the temperature corresponding to the specific heat peak ($T_p = 1.05$ – $1.07J$), there is no controversy about the nature of the transition. In the following subsections, we present and analyse results for the Penrose lattice, with a view to establishing similarity and distinction with respect to the periodic lattices.

3.1. Angular square displacement

The mean square angular displacement (henceforth referred to simply as the angular square displacement (ASD)) is a quantity which can indicate the existence or lack of long-range order. In 2D, one expects no long-range order and a logarithmic divergence of the ASD with the system length L . However, since the linear dimension L of a system is related to the number of sites N as $N \sim L^2$ in 2D, the divergence of the ASD with respect to N should also be logarithmic. In figure 2 we show the results for the ASD as a function of $\ln N$. These results were obtained by averaging over five blocks, each containing 14 000 spp. Although our values of $(7.09 \pm 0.07) \times 10^{-3}$ for the slope and $(1.04 \pm 0.05) \times 10^{-2}$ for the intercept are different to what is found for the square lattice ($m = 7.86 \times 10^{-3}$, $b = 5.52 \times 10^{-3}$) [7], this is to be expected, since these quantities are lattice dependent. The perfectly linear dependence of the ASD on $\ln N$ in figure 2 confirms the divergence of this quantity in the thermodynamic limit and indicates a lack of conventional ordering within our systems, thus ruling out any possibility of a second-order transition associated with the (dis)appearance of a spontaneous magnetization.

3.2. Specific heat

The results for the specific heat C , calculated from the fluctuations in the energy U of the system:

$$C = \frac{\langle U^2 \rangle - \langle U \rangle^2}{Nk_B T^2} \quad (2)$$

are shown in figure 3 for various system sizes, N . The saturation of the peak height with respect to system size and the smooth continuous variation of C with respect to temperature point to the absence of either a first- or a second-order transition. This behaviour, however, is consistent with a KT transition, for which C has an essential singularity at the critical temperature T_c . The specific heat in a KT transition remains smooth through the essential singularity at T_c and attains its maximum value at a temperature at which the correlation length is finite. For all system sizes larger than this correlation length, the specific heat remains unchanged. The general shape and features of the specific heat versus temperature curves shown in figure 3 agree well with those obtained for the square lattice [7, 8]. The only difference is the temperature T_p corresponding to the maximum in C . For our systems, we find $T_p = 1.10J$, whereas $T_p = (1.05$ – $1.07)J$ for the square lattice.

In using equation (2) to calculate C , one encounters a convergence problem in the peak region of $(1.0$ – $1.15)J$. Although we have been able to significantly improve these results by using five blocks of 200 000 spp within this region (and five blocks of 40 000–60 000 outside), our results are not accurate enough to allow us to comment definitively on the presence or absence of a cusp in C . As discussed by Van Himbergen and Chakravarty [8],

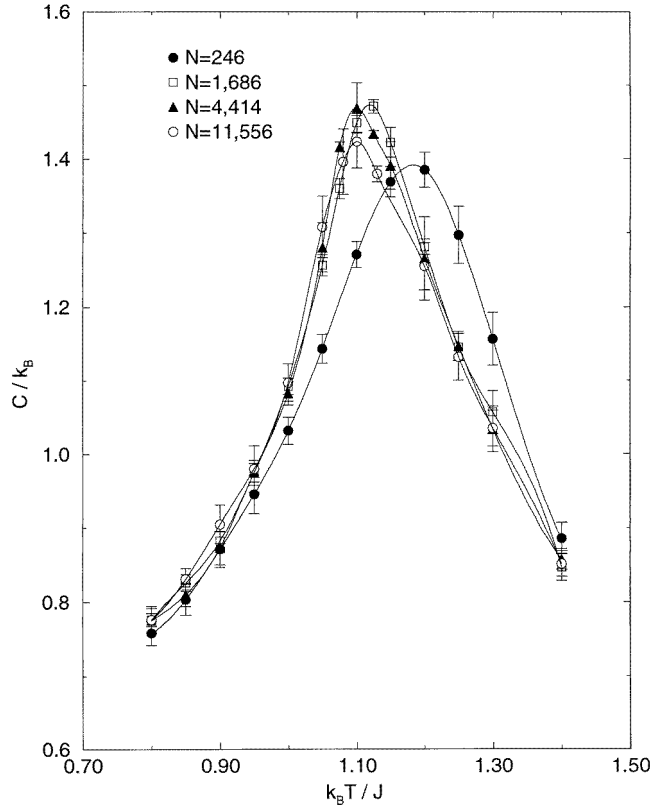


Figure 3. The specific heat (per particle), obtained via equation (2) for 2D periodic Penrose lattices (PPLs). The lines merely serve as guides for the eye. The $N = 246$ system is clearly below the saturation limit.

the presence of a cusp in C would imply an additional transition above the KT transition. These authors find that for the square lattice, the width of the specific heat peak narrows somewhat as the system size is increased. However, the largest lattice size considered by them is 1600. In our simulation, the narrowing rate seems to slow down for higher system size, e.g. between $N = 4414$ and $N = 11\,556$. Thus, the development of a cusp in the specific heat in the thermodynamic limit seems unlikely. We have repeated the specific heat calculation using the numerical derivative (of the energy) method. No feature other than a peak is revealed in the temperature variation of the specific heat.

3.3. Susceptibility

The linear susceptibility per spin is usually determined via the fluctuations in magnetization:

$$\chi = \frac{\langle m^2 \rangle - \langle m \rangle^2}{k_B T} \quad (3)$$

where m represents the magnetization per spin. Accurate determination of the thermal average of the magnetization, $\langle m \rangle$, in a numerical simulation has some inherent difficulties, as discussed extensively by Binder and Heermann [25]. However, for the 2D XY -model $\langle m \rangle$ can be shown analytically [26, 27] to be zero in the thermodynamic limit. This lack

of conventional ordering in our system is supported by our analysis of the ASD. Thus, to prevent any spurious value of $\langle m \rangle$ from affecting our results for χ , we have proceeded in the same fashion as Tobochnik and Chester [7] and set $\langle m \rangle = 0$ in equation (3).

Table 2. Comparison of results for the susceptibility χ of the 2D systems obtained via Metropolis and cluster algorithms. Only the cooling results are shown. Metropolis results represent averages over five blocks of 200 000 spp, whereas the cluster results were obtained by averaging over five blocks of 50 spp.

Temperature J/k_B	Susceptibility	
	Metropolis	Cluster
1.08	892 ± 101	931 ± 2
1.10	568 ± 59	540 ± 2
1.11	422 ± 42	418 ± 2
1.13	264 ± 27	256 ± 1
1.15	176 ± 5	171 ± 1
1.16	146 ± 4	141 ± 1

We find that with the Metropolis algorithm, it is difficult to obtain converged values of χ near T_c . We estimate that convergence within acceptable error bars under the Metropolis scheme would require extremely long runs on the SGI machines currently available to us. However, this convergence problem is eliminated by using the cluster algorithm of Wolff [20], and Ferrenberg and Swendsen [21]. As indicated in table 2, the cluster algorithm yields error bars for χ of $<0.5\%$. This is significantly better than the $\sim 10\%$ error bars obtained via the Metropolis algorithm. It appears that convergence in magnetization fluctuations is harder (more time consuming) to achieve via the Metropolis scheme for this particular 2D model. No such convergence problem was encountered for calculating the specific heat, where the two algorithms yielded similar results with similar error bars and within comparable cpu times. We refrain from making detailed comments about the relative advantages and disadvantages of the two algorithms, since our study is quite limited in this regard.

In figure 4, we present values of χ , obtained using the cluster algorithm. These results are for the $N = 11\,556$ system, and were calculated by averaging over five blocks of 50 spp.

For a KT transition, the susceptibility χ is expected to obey the following relation [13]:

$$\chi = \begin{cases} \sim \exp(bt^{-\nu}) & T > T_c \\ \infty & T \leq T_c \end{cases} \quad (4)$$

where $t = T/T_c - 1$. In figure 4, we present the results for χ for our largest system size $N = 11\,556$. The solid line is an exponential fit of the data points via equation (4), using the critical exponents $b = 1.5$ and $\nu = 0.5$, given by Kosterlitz [13]. Our estimate of T_c is 1.027 and the closest temperature to this that we are able to fit to our data to is 1.10, i.e. we are able to fit the data around temperatures that are only 7% away from the critical temperature. The KT form (equation (4)) holds for our data in the range 7–25% above T_c .

For values of $T \leq 1.08J$ we begin to see finite-size effects in the values of χ obtained from the simulation. The increase in χ becomes weaker than that given by the KT (exponential) form, approaching an N -dependent finite value at $T = 0$, while in an infinite lattice it is supposed to stay infinite below T_c . Equations involving finite-size scaling [28] involve only a logarithmic dependence on the system length L . As a result, one must examine very large systems, involving sufficiently different length scales. Such a scaling analysis,

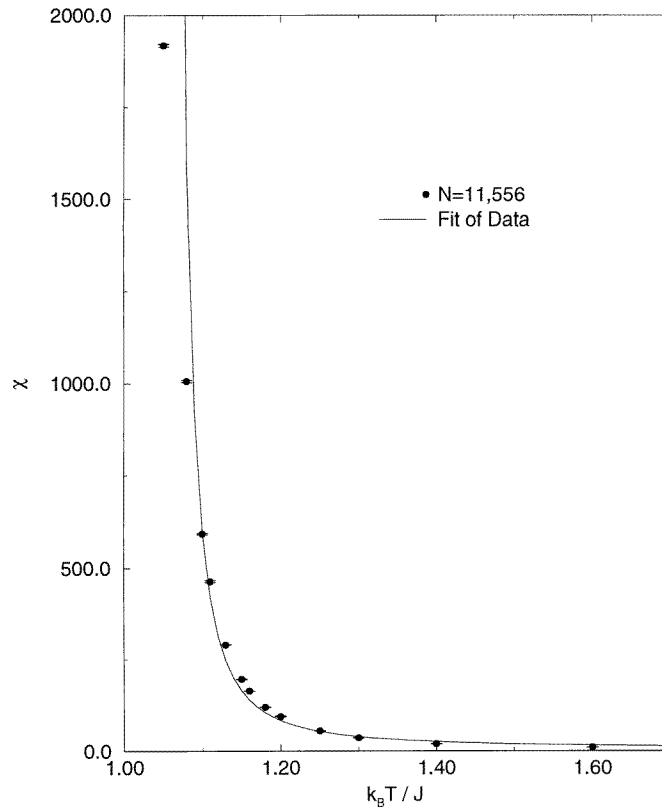


Figure 4. The susceptibility for the largest-size ($N = 11\,556$) 2D PPL used in this work. A fit using $\chi \sim \exp(bt^{-\nu})$, $b = 1.5$ and $\nu = 0.5$ over the temperature range $T = (1.10\text{--}1.30)J$ yields $T_c = (1.027 \pm 0.002)J$.

and therefore an independent derivation of the constants b and ν , lies beyond our present computing resources.

3.4. Helicity modulus

An important quantity in the study of the KT transition is the helicity modulus as discussed by Fisher, Barber and Jasnow [29]. It is a measure of the response of the system to an externally applied twist across its boundaries and plays a role similar to the shear or rigidity modulus in a solution \rightarrow gel or liquid \rightarrow solid transition. If we consider a two-dimensional system (of length L_x and width L_y) and apply periodic boundary conditions along, say, the y -axis, the helicity modulus, γ , can be determined from the difference between the free energies corresponding to anti-periodic and periodic boundaries along the x -axis [29, 8]:

$$F_a - F_p = \frac{\pi^2 L_y}{2 L_x} \gamma. \quad (5)$$

Below T_c the system will have some resistance to the twist; above T_c it will not. As the system is heated from an ordered state, γ will slowly decrease and will drop to zero at $T = T_c$.

In their study of granular superconductors, Shih, Ebner and Stroud [30] present a method of determining γ . Instead of imposing a twisted boundary condition, they add a term to the Hamiltonian (via the introduction of a vector potential), which is equivalent to applying a twist. The second derivative of the free energy with respect to this term yields the helicity modulus:

$$\gamma = N^{-1} \left[\sum_{\langle ij \rangle} J x_{ij}^2 \langle \cos(\theta_i - \theta_j) \rangle - \frac{1}{k_B T} \left\langle \left[\sum_{\langle ij \rangle} J x_{ij} \sin(\theta_i - \theta_j) \right]^2 \right\rangle + \frac{1}{k_B T} \left\langle \left[\sum_{\langle ij \rangle} J x_{ij} \sin(\theta_i - \theta_j) \right]^2 \right\rangle \right] \quad (6)$$

where N is the number of lattice sites and $x_{ij} = x_j - x_i$. Teitel and Jayaprakash, in their study of the frustrated XY-model [9], give an alternative expression for γ :

$$\gamma = -\frac{1}{2} \langle u \rangle - \frac{J^2}{k_B T N} \left\langle \left[\sum_{\langle ij \rangle} \sin(\theta_i - \theta_j) x_{ij} \right]^2 \right\rangle. \quad (7)$$

While there is some difference between these two equations, we have found that they yield similar results. For our simulations, we have used equation (7) to determine γ , primarily because it requires less CPU time.

In calculating γ , we have found that it is difficult to obtain converged values at high temperatures. Whereas five blocks of 5000 spp were sufficient at low temperatures, for $T > 0.8J$ many more steps were needed. In some cases, five blocks of over 150 000 spp were used (for $N = 4414$ and $T \geq 1.05J$).

According to Nelson and Kosterlitz [31, 32], the superfluid-to-normal transition in helium thin films can be interpreted as a KT transition, with γ being proportional to the superfluid density ρ_s . Nelson and Kosterlitz argue that there is a discontinuous drop of magnitude $2/\pi$ in γ at T_c , corresponding to the discontinuous drop in ρ_s at the transition. Our simulation results show (figure 5) a drop in γ at high temperature, which becomes sharper with increasing system size. The drop in γ for our 11 556-site lattice is the sharpest drop obtained so far in any numerical simulation on 2D lattices. We have analysed the size dependence of the slope of γ versus T curves, but lack of numerical precision prevents us from making a definite conclusion [33] regarding the nature (discontinuous versus continuous) and the magnitude (whether discontinuous or not) of the drop. On the basis of the location of the drop, we estimate a value of T_c in the range 1.0–1.05 J . This is in good agreement with the result $T_c = 1.027J$ obtained via the susceptibility fit.

Our results exhibit a low- T behaviour consistent with that obtained by Teitel and Jayaprakash for the square lattice [9] (namely: $\gamma \simeq J - k_B T/4$). The results for periodic lattices illustrate that as $T \rightarrow 0$, $\gamma \rightarrow -\frac{1}{2} \langle u \rangle$; where $\langle u \rangle$ is the average energy per particle [9, 10]. Thus, in our case, γ should approach unity. However, as figure 5 illustrates, γ approaches a value which is less than unity. This discrepancy can be explained by examining equation (7). We have found directly from our simulation that as $T \rightarrow 0$, the ensemble average in the second term on the right-hand side of equation (7) varies linearly with both N and T . Hence, at low temperatures, equation (7) can be rewritten as

$$\gamma = -\frac{1}{2} \langle u \rangle - \frac{J^2}{k_B T N} A k_B T N \quad (8)$$

or, more appropriately,

$$\gamma = -\frac{1}{2} \langle u \rangle - J^2 A \quad (9)$$

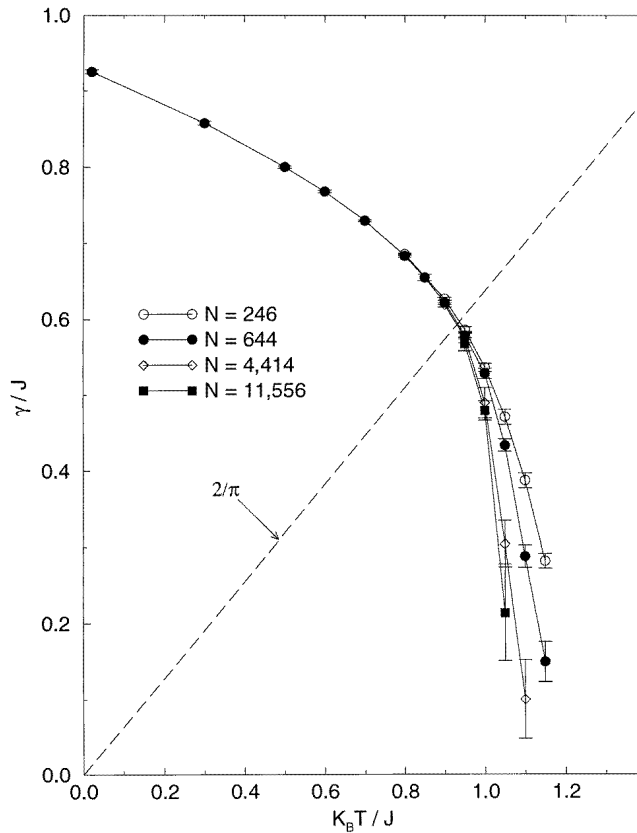


Figure 5. The helicity modulus for 2D PPLs. The lines presented serve as guides for the eye.

where the value of the constant A is lattice dependent. For regular periodic lattices the constant $A \rightarrow 0$ as $T \rightarrow 0$, but for the quasiperiodic lattices studied by us it seems to maintain a finite value. We have performed simulations of the helicity modulus on square lattices. These simulations show clearly that $\gamma \rightarrow 1$ as $T \rightarrow 0$, indicating that $A \rightarrow 0$ as $T \rightarrow 0$ for a square lattice.

Following Van Himbergen and Chakravarty [8] we have looked at the derivative $d\gamma/d\beta$, where β is the inverse temperature. This quantity can be related to the difference, $U_a - U_p$, between the energies of the system under anti-periodic and periodic boundary conditions (see equation (2.5) of reference [8]). The latter, and correspondingly $d\gamma/d\beta$, diverges at the KT transition temperature in the thermodynamic limit. For a finite lattice, $U_a - U_p$ has a peak at around the transition temperature and the height of the peak increases with the system size. Our simulation of this quantity for the system size 1686 shows a peak at $1.05J$. This value is slightly higher than the estimate of T_c from the susceptibility fit, but consistent with the T_c -range given by the helicity modulus itself. If there is a slight downward shift in the peak location with increasing system size, as observed for the square lattice [8], the asymptotic value of T_c would be more in line with the value $T_c = 1.027J$, obtained from the fit to the susceptibility. Since the numerical problems associated with computing this quantity increase significantly with the system size, lattices of larger size were not considered.

Table 3. The number of sites and linear dimensions of the 3D systems used in the simulation.

N	L_x	L_y	L_z
42	3.62	3.08	3.0
752	9.47	8.06	8.0
3198	15.33	13.04	13.0
13 524	24.80	21.10	21.0
57 324	40.12	34.13	34.0

4. 3D systems

To create 3D systems, we have stacked 2D PPLs periodically along the z -axis (ensuring that each plane is identical). Since the PPLs are rectangular, we cannot create completely cubic boundaries. However, we have kept the overall length of the systems in the z -direction similar to that in the y -direction in an effort to give them a nearly cubic shape. We have kept the interplanar nn spacing equal to the intraplane nn distance (unity). Although spins are still confined to the xy -plane, spins in plane π_i are now allowed to interact with those in planes π_{i+1} and π_{i-1} (with $J = 1$ for both interplanar and intraplanar interactions). In table 3, we present the dimensions of the systems which were used for these simulations.

Periodic boundary conditions were utilized for all of the directions, x , y and z . Starting from a high-temperature ($T = 3.0J$) random configuration, the systems were cooled in a quasistatic manner to a temperature of $T = 1.0J$. They were then reheated, back to the high-temperature limit, in the same fashion. Using the Metropolis algorithm [19], five blocks of 15 000 spp were sufficient for calculating the averages above and below the transition, whereas in the T_c -region, five blocks of 25 000 spp were used.

Table 4. Critical exponents for the 3D XY-model, as given in reference [17], and as obtained in this work for a periodic stacking of 2D Penrose lattices.

Quantity	Exponent	Value from Betts (reference [17])	Value obtained in this work
Specific heat	α	0	0.03 ± 0.03
Magnetization	β	1/3	0.30 ± 0.01
Susceptibility	γ	4/3	1.31 ± 0.02

Previous Monte Carlo studies using cubic systems [14–16] all confirm a second-order phase transition occurring at $T_c = 2.20J$. Furthermore, the critical exponents that they obtain are also in good agreement with those obtained from other methods [17]. These exponents (as given by Betts [17]) are summarized in table 4. We have examined the spontaneous magnetization m , susceptibility χ and specific heat C . Our results and analysis are presented in the following subsections.

4.1. Magnetization

The spins in a finite system have a tendency to undergo global rotation, thus spuriously lowering the value of the magnetization. As discussed by Binder and Heermann [25], in such situations one must calculate $\langle |m| \rangle$ as opposed to $\langle m \rangle$. We have followed this prescription for estimating the magnetization. While we have actually calculated $\langle |m| \rangle$, we shall henceforth refer to this quantity simply as m .

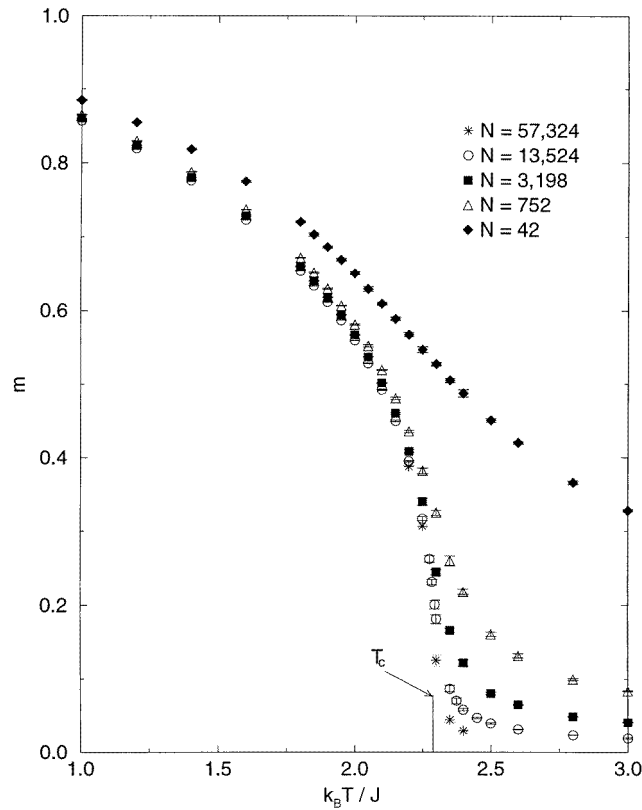


Figure 6. Magnetization in the 3D periodic stacking of 2D PPLs. Note the attenuation of the tail region with increasing system size.

As figure 6 illustrates, the behaviour of m for our system is, indeed, consistent with a second-order phase transition. At low temperatures ($T \sim 1.0J$), we see the onset of strong ferromagnetic ordering, with m tending to unity at $T = 0$. Upon heating the system, the magnetization decreases and approaches zero in the high-temperature region. Our results show the typical temperature variation of the order parameter in a second-order phase transition, as obtained in various previous numerical studies (such as those for the 2D and 3D Ising models [25, 34]). For smaller systems the order parameter goes to zero with an extended tail. The tail region steadily diminishes with the increasing system size. For our largest size, $N = 57\,324$, the tail region or the finite-size effect seems to be remarkably small.

We have performed the cumulant analysis, given by Binder [25, 35, 36], to accurately determine the value of T_c for our system. We computed the fourth-order cumulant U_L , given by

$$U_L = 1 - \frac{\langle m^4 \rangle_L}{3\langle m^2 \rangle_L^2}. \quad (10)$$

At $T = T_c$, U_L reaches a fixed value for all L . By determining U_L for various lattice sizes and calculating the ratio $U_L/U_{L'}$, one is able to determine T_c from a plot of the different $U_L/U_{L'}$ curves. This analysis is presented in figure 7. The various curves

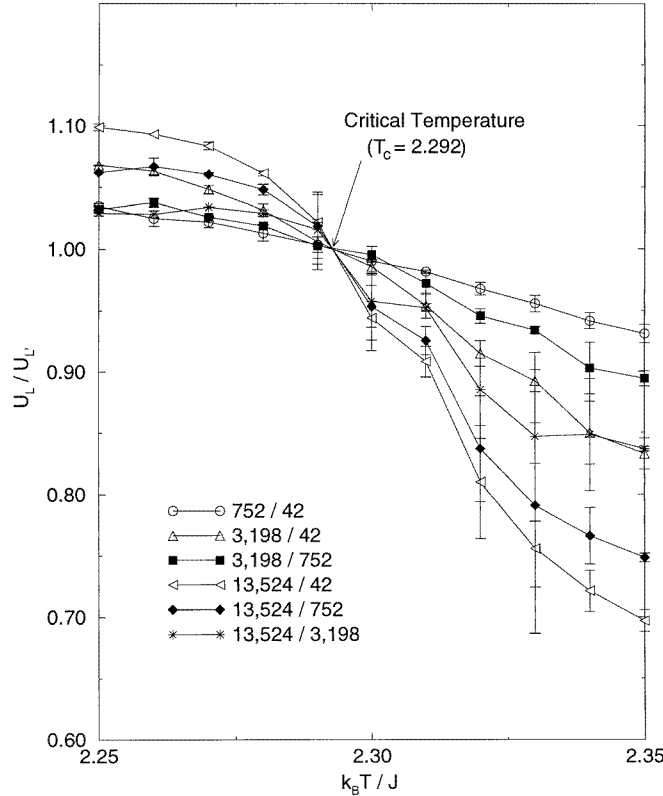


Figure 7. The determination of T_c for the 3D systems using cumulant ratios. The $U_L/U_{L'}$ for various systems all indicate $T_c = (2.292 \pm 0.003)J$.

intersect at $U_L/U_{L'} = 1$ and the temperature at which this occurs is the critical temperature: $T_c = 2.292J$.

With this value of T_c , it is possible to perform a finite-size scaling analysis of m , in an effort to determine its critical exponent β . The appropriate scaling relation is [25, 34]

$$m = N^{-\beta/3\nu} \hat{f}[(T - T_c)N^{1/3\nu}] \quad (11)$$

where \hat{f} is the finite-size scaling function, ν is the critical exponent describing the power-law decay of the correlation length and we have estimated the linear dimension L by $N^{1/3}$. Because of the finite-size effects and the periodic boundary conditions, reliable values of the correlation length are difficult to obtain. The problem is even greater close to the transition, making it almost impossible to determine ν from a direct computation of the correlation length. Instead of computing the correlation length, we have studied the scaling plots of the cumulants U_L as functions of $(T - T_c)L^{1/\nu}$, with $T_c = 2.292J$, given by the crossing of the cumulants. Depending on whether we choose L_x , L_y , L_z or $N^{1/3}$ as L and the number of temperature values close to T_c that we include in the plot, we obtain values of ν ranging between 0.6 and 0.7. The accepted value of ν for the 3D XY-model, obtained from the studies on cubic lattices, is $2/3$ [17], within the range of values that we obtain from the above scaling plots. We thus assume $\nu = 2/3$ and use this value of ν to obtain the magnetization exponent β . With $x = (T - T_c)N^{1/3\nu}$ and $y = mN^{\beta/3\nu}$ we obtain a plot of y versus x . When this is done with the correct choice of ν , T_c and β , the values of m

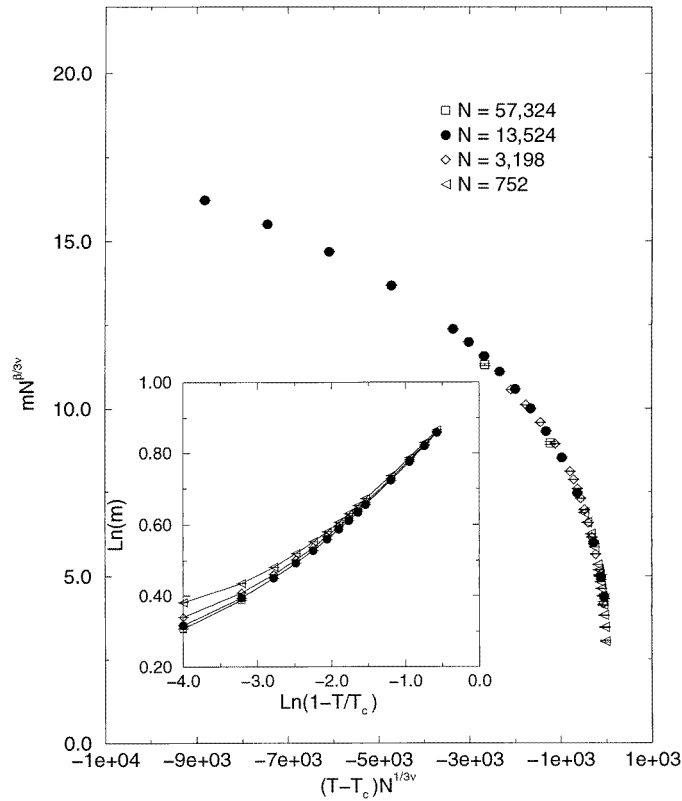


Figure 8. Finite-size scaling analysis of m . Using $\nu = 2/3$ and $T_c = 2.292J$, the data can be collapsed onto a single curve with $\beta = 0.3$. The inset illustrates the increase in β with the system size near T_c .

for the various system sizes should all collapse onto a single curve. For our systems we find that the best fit occurs for $\beta = 0.3$ (with $\nu = 2/3$ and $T_c = 2.292$). This value of β is slightly lower than the value $1/3$ given in table 4. However, we note a clear trend in the $\ln m$ versus $\ln(1 - T/T_c)$ plot for our systems (in the inset of figure 8). This graph indicates that the slope of the lines (and thus β) increases with the system size as one approaches T_c (the -3 to -4 region). Therefore, for larger lattices we should be able to obtain values of β slightly higher than 0.3 , which we hope will saturate to the value $1/3$ in the infinite-lattice limit.

4.2. Susceptibility

Our results for χ are also consistent with a second-order phase transition (figure 9). They show no saturation with the system size, pointing to a divergence in the thermodynamic limit. For finite-size systems, χ satisfies the scaling relation

$$\chi = N^{\gamma/3\nu} \hat{g}[(T - T_c)N^{1/3\nu}] \quad (12)$$

where γ is the susceptibility exponent and \hat{g} is the scaling function. We have analysed this relationship for both $T > T_c$ and $T < T_c$. For reference purposes, we denote γ as the exponent which describes the behaviour when $T > T_c$ and γ' that for $T < T_c$.

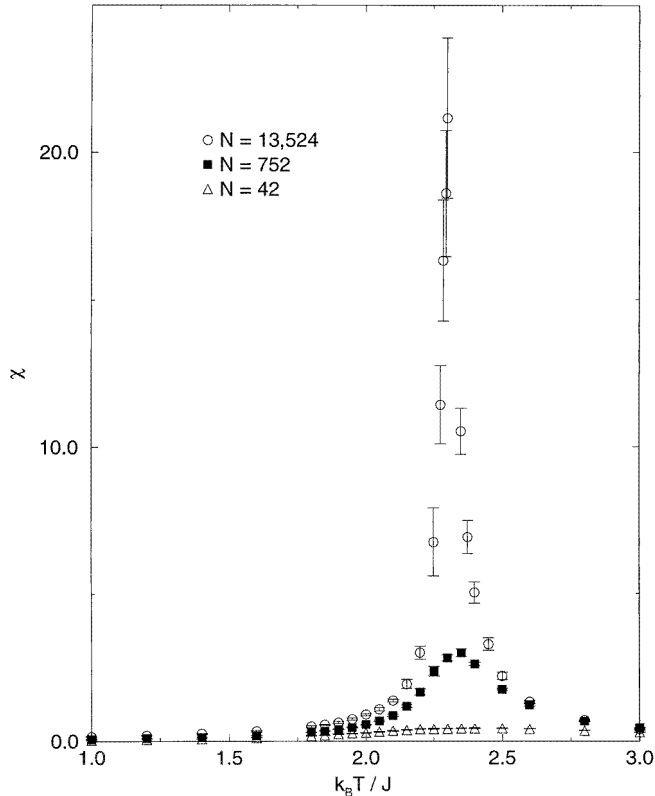


Figure 9. The susceptibility in the 3D systems, showing a lack of saturation and a divergence with increasing system size, consistent with a second-order transition.

The result of this analysis (for both cases) is given in figure 10. For $T > T_c$, we obtain the best fit when $\gamma = 1.30$. For $T < T_c$, we find that this occurs when $\gamma' = 1.33$. Although one should obtain $\gamma = \gamma'$, the difference is not unusual, when compared with previous studies of χ . These studies find values for γ ranging from $4/3$ [17] to 1.30 [24]. The results obtained via the MC studies on cubic lattices all fall within this range. Thus, even though our values for γ and γ' are not equal, they are in good agreement with previous work on cubic lattices.

4.3. Specific heat

Our results for the specific heat, C , are displayed in figure 11. There is no saturation with respect to the system size. The divergence in specific heat becomes apparent for our largest size, $N = 13\,524$. One can conduct a finite-size scaling analysis in an effort to determine the specific heat exponent α . However, there are severe numerical problems associated with determining α , due to its extremely small value. The divergence in the specific heat at T_c is almost logarithmic, with α being close to zero. The value quoted in the review article by Betts [17] is exactly zero, while Yeomans [24], in her textbook on phase transitions, quotes a value of 0.01 . Estimates of α from high-temperature series expansion, experimental work on ^4He near the superfluid transition and field-theoretical methods have been discussed

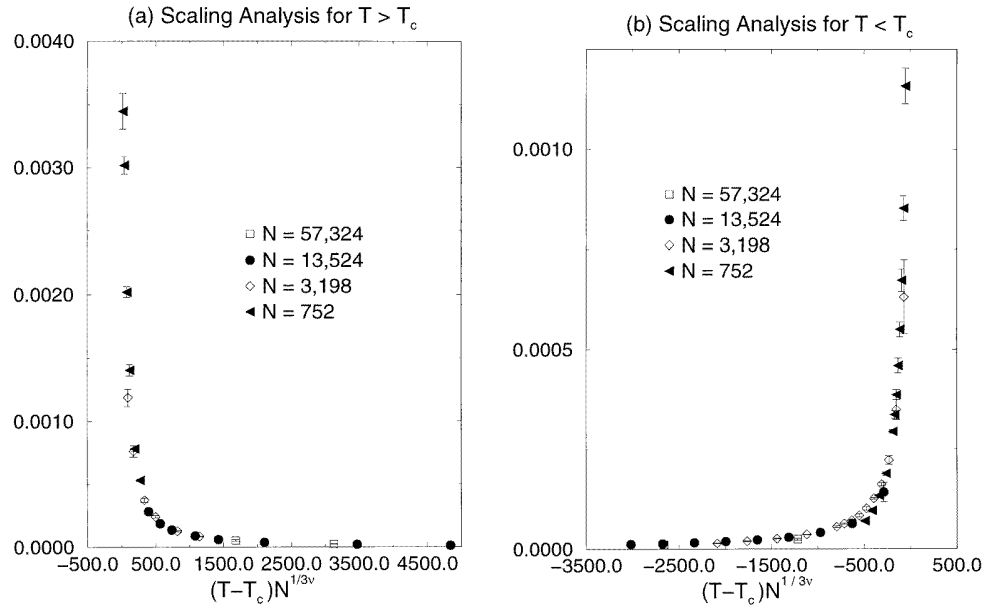


Figure 10. Finite-size scaling analysis of the susceptibility. Using $\nu = 2/3$ and $T_c = 2.292J$, one obtains: (a) $T > T_c$, $\gamma = 1.30$; (b) $T < T_c$, $\gamma' = 1.33$.

by Brass and Mitrović [37]. All of these estimates border around zero. Note that the Rushbrooke's hyperscaling relation [38], $\alpha + 2\beta + \gamma = 2$, indicates a value of $\alpha = 0.1$, if we use $\gamma = 1.30$ and $\beta = 0.3$ for our system. This is an upper limit, since our results also permit using $\gamma = 1.33$ and $\beta = 0.33$, which would yield $\alpha = 0.01$ in agreement with reference [24]. Josephson's hyperscaling relation, $\nu d = 2 - \alpha$, should yield $\alpha = 0$ for $d = 3$, if we assume $\nu = 2/3$. Our finite-size scaling results indicate a value close to 0.3. This, we think, is due to the fact that small errors in the simulated values of the specific heat close to T_c can give rise to large changes in the exponent, when the exponent is close to zero.

Through a plot of $\ln C$ versus $\ln(1 - T/T_c)$, we have been able to establish a somewhat meaningful value of α' for our $N = 13\,524$ system. As figure 12 indicates, near T_c , where the relation $c \sim |t|^{-\alpha}$ is supposed to hold, the slope of the data (and thus α') is quite small. In fact, this yields a value of $\alpha' \sim 0.03$, which is considerably better than the value obtained from the finite-size scaling analysis. We have been unable to determine α for the $T > T_c$ case using this method. Our (inadequate) system size seems to have a stronger influence on the data in this region, making it less reliable than the data for $T < T_c$ by a similar amount.

4.4. Summary of 3D results

In table 4 we provide our most reliable estimates, along with the error bars, of the specific heat, magnetization and the susceptibility exponents, and compare them with the accepted values for the 3-D XY-model in the literature [17]. As discussed in the previous subsections, our estimates of the specific heat, and the susceptibility exponents have small differences in their values above and below the transition. The error bars in table 4 are obtained from the fitting of the simulated quantities to the power-law form near the transition.

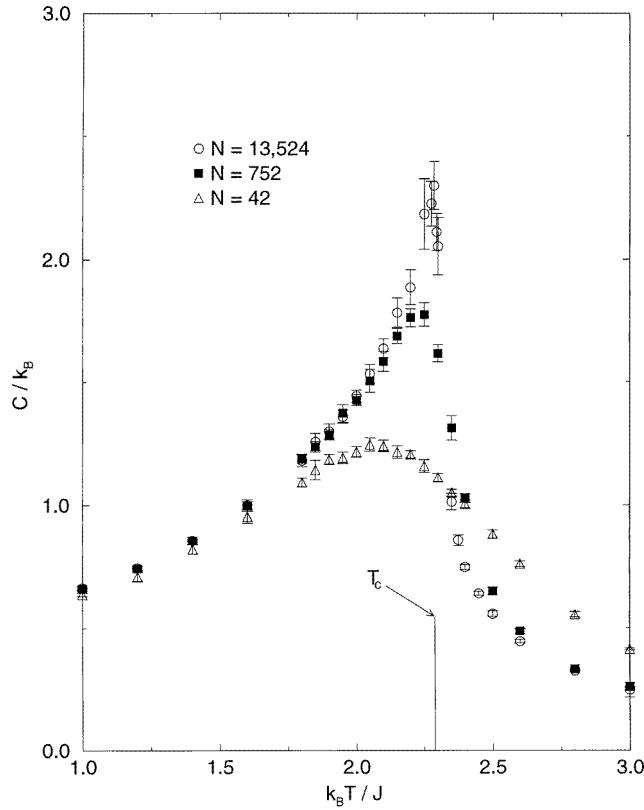


Figure 11. Like χ , C has a divergence consistent with a second-order transition.

5. Comments and conclusion

Through our analysis of the specific heat, susceptibility and helicity modulus, we have conclusively shown that the XY-model on a 2D Penrose lattice exhibits a Kosterlitz–Thouless transition. Our numerical simulation points to a KT transition occurring in the temperature range $T_c = (1.0\text{--}1.05)J$, while the specific heat peak is at $T_p = 1.10J$. These values are slightly higher than the values $T_c = (0.89\text{--}0.95)J$ and $T_p = (1.05\text{--}1.07)J$ for the square lattice [7–10]. However, the overall behaviour of the susceptibility, specific heat and helicity modulus in our simulation is remarkably similar to that reported for the latter. Furthermore, our data are consistent with the critical exponents $b = 1.5$ and $\nu = 0.5$, reported in the original Kosterlitz–Thouless work [12, 13].

For a 3D stacking of the 2D Penrose lattices we find that the system undergoes a classical second-order transition, with magnetization as the order parameter. This behaviour is supported by our analysis of the magnetization, susceptibility and specific heat. Like the 2D results, the critical temperature of $T_c = (2.292 \pm 0.003)J$ for our system is slightly higher than that found for cubic systems. The higher values of T_c for both our 2D and 3D systems (compared with those for the square and the cubic lattices, respectively) are most probably due to the variation in coordination number from site to site. Although the average coordination number for the 2D Penrose lattice is the same as for the square lattice, the actual coordination number varies between 3 and 7. The critical exponents $\alpha' = 0.03 \pm 0.03$,

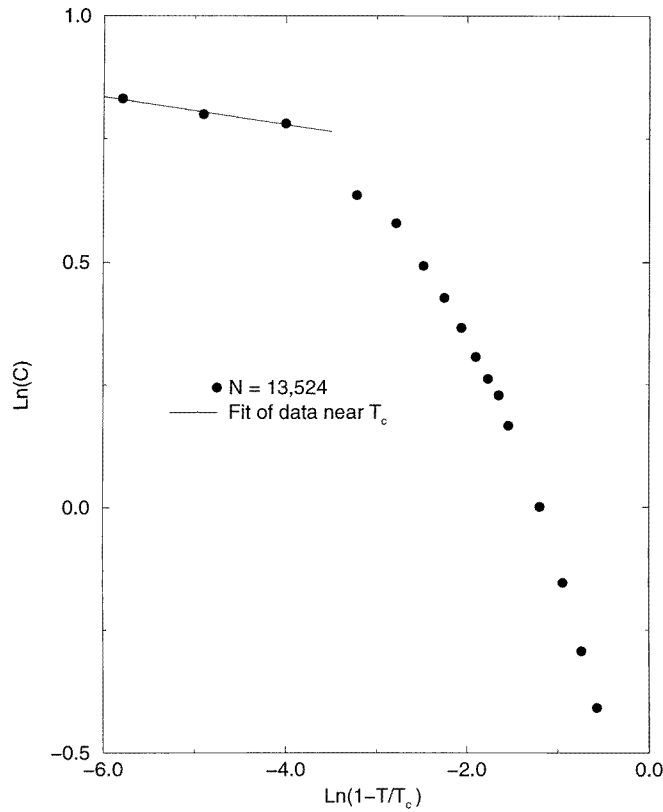


Figure 12. A plot of $\ln C$ versus $\ln(1 - T/T_c)$. One can determine the value of α' from the slope of the data near T_c . In this case, $\alpha' = 0.03$.

$\beta = 0.30 \pm 0.01$ and $\gamma = 1.31 \pm 0.02$ are in good agreement with accepted values for the 3D XY-model, indicating that the periodic and the quasiperiodic lattices belong to the same universality class for this model.

Acknowledgment

Financial support for this work was provided by the Natural Sciences and Engineering Research Council of Canada.

References

- [1] Luck J M 1993 *Europhys. Lett.* **24** 359
- [2] Sorensen E S, Jarić M V and Rochetti M 1991 *Phys. Rev. B* **44** 9271 and references therein
- [3] Zhang C and De'Bell K 1993 *Phys. Rev. B* **47** 8558 and references therein
- [4] Langie G and Iglói F 1992 *J. Phys. A: Math. Gen.* **25** L487 and references therein
- [5] Korepin V E 1987 *Commun. Math. Phys.* **100** 157
- [6] Strandburg K J 1991 *Comput. Phys.* **5** 520
- [7] Tobochnik J and Chester G V 1979 *Phys. Rev. B* **20** 3761
- [8] Van Himbergen J and Chakravarty S 1981 *Phys. Rev. B* **23** 359
- [9] Teitel S and Jayaprakash C 1983 *Phys. Rev. B* **27** 598

- [10] Shih W and Stroud D 1984 *Phys. Rev. B* **30** 6774
- [11] Ledue D, Teillet J, Carnet J and Dujardin J 1993 *J. Non-Cryst. Solids* **153+154** 403
- [12] Kosterlitz J M and Thouless D J 1973 *J. Phys. C: Solid State Phys.* **6** 1181
- [13] Kosterlitz J M 1974 *J. Phys. C: Solid State Phys.* **7** 1046
- [14] Hasenbusch M and Meyer S 1990 *Phys. Lett.* **241B** 238
- [15] Janke W 1990 *Phys. Lett.* **148A** 306
- [16] Gottlob A and Hasenbusch M 1993 *Physica A* **201** 593
- [17] Betts D D 1974 *Phase Transitions and Critical Phenomena* vol 3, ed C Domb and M S Green (New York: Academic) pp 569–652
- [18] Burkov S E 1991 *Phys. Rev. Lett.* **67** 614
- [19] Metropolis N C, Rosenbluth A W, Rosenbluth M N and Teller E 1953 *J. Chem. Phys.* **21** 1087
- [20] Wolff U 1989 *Phys. Rev. Lett.* **62** 361
- [21] Ferrenberg A M and Swendsen R H 1989 *Phys. Rev. Lett.* **63** 1195
- [22] Lançon F and Billard L 1986 *Europhys. Lett.* **2** 625
- [23] Plischke M and Bergersen B 1989 *Equilibrium Statistical Physics* (Englewood Cliffs, NJ: Prentice-Hall)
- [24] Yeomans J M 1992 *Statistical Mechanics of Phase Transitions* (New York: Oxford University Press)
- [25] Binder K and Heermann D 1992 *Monte Carlo Simulation in Statistical Physics* (New York: Springer)
- [26] Mermin N D and Wagner H 1966 *Phys. Rev. Lett.* **17** 1133
- [27] Wegner F 1967 *Z. Phys.* **206** 465
- [28] Szeto K Y and Dresselhaus G 1985 *Phys. Rev. B* **32** 3142
- [29] Fisher M E, Barber M N and Jasnow D 1973 *Phys. Rev. A* **8** 111
- [30] Shih W Y, Ebner C and Stroud D 1984 *Phys. Rev. B* **30** 134
- [31] Nelson D and Kosterlitz J 1977 *Phys. Rev. Lett.* **39** 1201
- [32] Nelson D R 1983 *Phase Transitions and Critical Phenomenon* vol 7, ed C Domb and J L Lebowitz (New York: Academic)
- [33] We estimated the slope towards the rightmost sections of the curves. Given the error bars in the results and the mesh size, these are crude estimates. We do find that the slope $P \sim A \ln(N)$, with A lying between 0.25 and 0.26. There is a small intercept, but considering the uncertainties in our estimates of P for the four N -values, we consider this as a fair indication that the slope goes to infinity in the thermodynamic limit. Since the slopes refer to the parts of the curves before the zero value of the helicity modulus is reached, we infer that the drop is discontinuous in the thermodynamic limit. However, since we have only four data points over a range of N which is admittedly narrow on the logarithmic scale, the above conclusion stands on shaky grounds. The magnitude of the discontinuity also remains uncertain.
- [34] Mouritsen O G 1984 *Computer Studies of Phase Transitions and Critical Phenomena* (Berlin: Springer)
- [35] Binder K 1981 *Z. Phys. B* **43** 119
- [36] Binder K 1981 *Phys. Rev. Lett.* **47** 693
- [37] Brass A and Mitrović B 1991 *Physica C* **177** 138
- [38] Stanley H E 1971 *Introduction to Phase Transitions and Critical Phenomenon* (New York: Oxford University Press)